Chinese Journal of Oceanology and Limnology
Vol. 28 No. 5, P. 1021-1028, 2010
DOI: 10.1007/s00343-010-9056-8

Measurements of ocean wave and current field using dual polarized X-band radar*

CUI Limin (崔利民)[1,2,3], HE Yijun (何宜军)[1,2,**], SHEN Hui (申辉)[1,2], LÜ Haibin (吕海滨)[1,2,3,4]

[1] *Institute of Oceanology, Chinese Academy of Sciences, Qingdao 266071, China*

[2] *Key Laboratory of Ocean Circulation and Wave, Chinese Academy of Sciences, Qingdao 266071, China*

[3] *Graduate University of the Chinese Academy of Sciences, Beijing 100039, China*

[4] *School of Geodesy and Geomatics Engineering, Huaihai Institute of Technology, Lianyungang 222005, China*

Received Oct. 28, 2009; revision accepted Mar. 19, 2010

Abstract A new ocean wave and sea surface current monitoring system with horizontally-(HH) and vertically-(VV) polarized X-band radar was developed. Two experiments into the use of the radar system were carried out at two sites, respectively, for calibration process in Zhangzi Island of the Yellow Sea, and for validation in the Yellow Sea and South China Sea. Ocean wave parameters and sea surface current velocities were retrieved from the dual polarized radar image sequences based on an inverse method. The results obtained from dual-polarized radar data sets acquired in Zhangzi Island are compared with those from an ocean directional buoy. The results show that ocean wave parameters and sea surface current velocities retrieved from radar image sets are in a good agreement with those observed by the buoy. In particular, it has been found that the vertically-polarized radar is better than the horizontally-polarized radar in retrieving ocean wave parameters, especially in detecting the significant wave height below 1.0 m.

Keyword: dual polarization; X-band radar; sea state parameters; current field

1 INTRODUCTION

Conventional X-band nautical radar can measure ocean waves and the ocean current field from radar backscatter images (Young et al., 1985). Commercial wave monitoring systems, such as WaMoS II and WAVEX, have been developed based on a modification of the HH-polarization nautical radar (Young et al., 1985; Nieto et al., 2000). The LGA (low grazing angle) ocean clutter exhibits fairly complex behavior, and many of its aspects are still not well understood, and cannot be precisely predicted (Brown, 1998). Hwang et al. (2008a) assumed that the intensity of radar backscatter from the ocean surface at low grazing angles is much stronger than theoretical computations, especially for horizontal polarization. Many works have been published on radar backscatter with grazing angle for both polarizations. Lee et al. (1995) indicated that non-Bragg scattering contributes noticeably to the returns of both polarizations, but is dominant in providing returns for the horizontal polarization. Trizna et al. (1996) noted differences between HH and VV polarized radar returns in the coastal environments of Bermuda and La Jolla in light to moderate winds and in the absence of long gravity waves. Images from the HH polarization show a more discrete character while those from the VV polarization show a more spatially homogeneous texture. They proposed that the differences in the spatial texture reflect the differences in the scattering mechanisms for the two polarizations: evenly distributed Bragg scatter patches for VV and spiky scatter from small asymmetric bore features for HH. Forget et al. (2006) performed some experiments on L-band radar considering two polarizations in a Mediterranean coastal zone, and suggested that at low grazing angles, non-Bragg scattering effects play a major role in horizontal polarization, especially under high-wind-high-wave conditions. Hwang et al.

* Supported by the Knowledge Innovation Program of the Chinese Academy of Sciences (Nos. KZCX1-YW-12-04, KZCX2-YW-201), and the Instrument Developing Project of the Chinese Academy of Sciences (No. YZ200724)

** Corresponding author: heyj@qdio.ac.cn

(2008b) reported that the non-Bragg scattering events with a back scattering cross section of horizontal polarization exceed that of the vertical polarization at low grazing angle by analyzing the field data sets.

Young et al. (1985) showed that the spectral analysis of a radar image sequence yields valuable information on both the surface wave field and the near surface currents. During the last two decades, inversion technology of estimating waves and current has been improved. Senet et al. (2001) applied an iterative technique to increase the accuracy of the current velocity. The estimation method for a surface current was also improved based on the consideration of nonlinear structures and correction for temporal undersampling (aliasing) (Seemann et al., 1997). In addition, significant wave height cannot be directly determined from radar images. The idea to obtain wave height information from SAR image was first applied to a radar image sequence by Ziemer et al. (1994). Borge (2004) derived a modulation transfer function based on a numerical simulation and further estimated the wave spectrum from radar imaging. Ren et al. (2006) obtained the wave parameters from a radar image using two-dimensional cross- and auto-correlation functions. Li et al. (2006) indicated that the key to retrieve the arithmetic is the analysis of the modulation mechanism based on the field experiment. In fact, the X-band radar not only may estimate the wave parameter and surface current, but also may determine wave groups (Dankert et al., 2003), wind field and bathymetry in inhomogeneous areas like coastal zones or areas with current gradients (Dankert, 2003). Bell (1999, 2001) and Bell et al. (2006) used X-band radar as a tool for remote mapping of bathymetry in a variety of locations on open coastlines. Dankert retrieved wind speed based on analyzing the movement of wind gusts using optical flow method (OFM) (2004) and the neural networks method (NNs) (2005). The analysis method for determining radar image spectra has also improved. A wavelet transform technique was applied to radar images of the inhomogeneous wave field (Doong, 2003). Although the inversion method is under developing, the method is able to make use of existing radar data sets from HH polarization. Due to the different imaging mechanisms for HH and VV polarizations described above, we developed a radar system with dual polarizations. The polarization influence on the estimation of the sea state parameters and sea surface current was studied. In this paper, we descriped the methods and experiments, and compared the ocean wave parameters and sea surface currents retrieved from X-band radar image sets by considering the observations of in-situ pitch roll buoy and current meters.

2 METHODS

The measurement of waves and currents with X-band radar is based on the spatial and temporal structure analysis of radar images of the sea surface. Radar images are acquired by radar reflection from the sea surface at low grazing angles. However, the radar images do not map ocean surface elevation on a one-to-one scale. Therefore, to estimate ocean wave parameters and current fields, an inverse modeling technique is needed. This method is based on the estimation of three-dimensional wave number/frequency spectra using three-dimensional fast Fourier transforms.

For a linear gravity wave, the sea surface is dispersive under the dependence between the wave number k and the angular frequency ω Eq.1. The dispersion is deformed by the Doppler speed (Fig.1). Under the assumption of a linear gravity wave, the energy associated with the ocean waves is extracted from the image spectrum by first estimating the surface current and then applying the dispersion relation as a band-pass filter (Young et al. 1985). To correct for the effects of shadowing and tilt modulation on radar imaging, the wave spectrum was implemented from the filtered two-dimensional image spectra by applying a Modulation Transfer Function (MTF) (Ziemer et al., 1987).

$$\omega = \sqrt{gk \tanh(kh)} + kU \tag{1}$$

where g is the acceleration of gravity, h is the water depth, $k = |k|$ is the wave number and $U = (U_x, U_y)$ is the surface current speed.

2.1 The near surface current retrieval

Young et al. (1985) have proposed an algorithm, based on a least squares regression method, to determine the velocity of an encounter. A theoretical dispersion shell is fitted to the signal coordinates of the linear surface waves in the 3-D spectrum. Gangeskar (2002) used the same idea and derived a cost function, as in Eq.2, to estimate the current speed and direction.

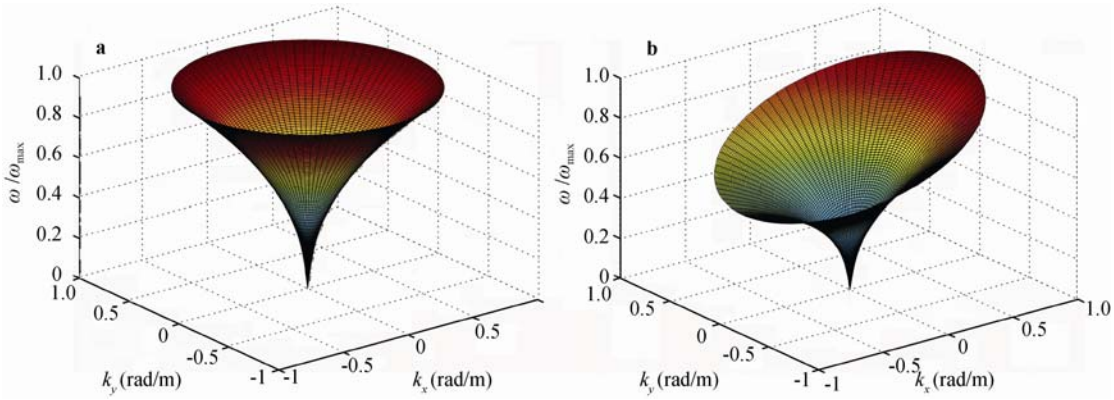

Fig.1 Dispersion relation with no current (a) and with current (b)

$$J=\sum_{\omega=0}^{\omega_N}\sum_{k_x=-k_{xN}}^{k_{xN}}\sum_{k_y=-k_{yN}}^{k_{yN}}\left(\Delta\omega\right)^2 E(k_x,k_y,\omega)=\min \qquad (2)$$

where

$$\Delta\omega=\omega-\sqrt{g\left|\vec{k}\right|\tanh\left(\left|\vec{k}\right|h\right)}-k_x u_x-k_y u_y$$

By minimizing the cost function, the current can be estimated by Eq.3:

$$\begin{bmatrix}u_x\\u_y\end{bmatrix}=\begin{bmatrix}\sum Ek_x^2 & \sum Ek_xk_y\\ \sum Ek_xk_y & \sum Ek_y^2\end{bmatrix}^{-1}\cdot \begin{bmatrix}\sum Ek_x\left(\omega-\sqrt{g\left|\vec{k}\right|\tanh\left(\left|\vec{k}\right|h\right)}\right)\\ \sum Ek_y\left(\omega-\sqrt{g\left|\vec{k}\right|\tanh\left(\left|\vec{k}\right|h\right)}\right)\end{bmatrix} \qquad (3)$$

Regression technology is applied to the estimation of the current and improves the accuracy significantly. More details of about regression method were given by Senet (2001).

2.2 Sea state parameters retrieval

The wave height information is not obtained directly from the radar. Significant wave height is statistically determined from the radar image spectra using Eq.4. It is based on the assumption that the square-root of the measured signal-to-noise ratio (SNR) is linearly related to significant wave height.

$$H_s = A + B\sqrt{SNR} \qquad (4)$$

Here A and B are calibration constants. The SNRs for nautical radar images were obtained from the image spectrum by means of a dispersion relation (Ziemer et al., 1994).

Other sea state parameters, such as dominant wave direction and average period, can be derived from the ocean wave spectra. The radar ocean wave spectrum E (k_x, k_y) is obtained from the radar image spectrum using the empirical MTF. To obtain the one-dimensional frequency spectrum, the frequency direction spectrum can be transferred from the wave number spectrum using Eq.5.

$$E(f,\theta)=JE(k_x,k_y) \qquad (5)$$

where J, the Jacobian coefficient, has the form of:

$$J=\left\{\frac{1}{2\pi}\left|\vec{k}\right|\frac{\mathrm{d}\left|\vec{k}\right|}{\mathrm{d}\omega}\right\} \qquad (6)$$

The one-dimensional frequency spectrum is computed by Eq.7:

$$S(f)=\int_0^{2\pi}E(f,\theta)\mathrm{d}\theta \qquad (7)$$

The mean period is given by Eq.8, according to the theory of random waves:

$$\overline{T}=\sqrt{\frac{\int_0^{f_N}S(f)\,\mathrm{d}f}{\int_0^{f_N}f^2S(f)\,\mathrm{d}f}} \qquad (8)$$

The main wave direction is inferred as:

$$\theta_p=\theta(f_p) \qquad (9)$$

where f_p is the location of the energy maximum with $S(f)$.

3 EXPERIMENT DESCRIPTIONS

Experiments were implemented in two areas. A calibration experiment was carried out on Zhangzi Island and validation was undertaken in the South China Sea.

3.1 Zhangzi Island calibration experiment

The radar antenna was operated in the X-band

(9.4 GHz) with VV (vertical transmit and vertical receipt) polarization and HH (vertical transmit and vertical receipt) polarization. It was positioned on the northwest corner of Zhangzi Island (located at 39°N, 122°E), at a height above mean sea level of approximately 35 m. The antenna rotation period was about 2.5 s. The imaged area was homogeneous with a depth of about 35 m.

Additionally, a pitch-roll buoy (SZF), developed by Ocean University of China, and the current meter (COMPACT-EM), developed by the ALEC Co. of Japan, were mounted about 1 km off the coast. The buoy sampled once every 3 hours during which time it recorded about 17 min of continuous data consisting of a time series of 2 048 points with a sampling interval of 0.5 s. In addition, the current meter was mounted 3 m under the water close to the buoy. The current meter recorded 10 sample points over 20 s each half hour.

3.2 South China Sea validation experiment

The presented data sets were obtained during the field investigation cruise of the Knowledge Innovation Program of the Chinese Academy of Sciences (No. KZCX1-YW-12) in the South China Sea (SCS). The radar system was mounted aboard the research vessel "*Kexue No.1*". The radar equipment used for this experiment was the same as that used at Zhangzi Island. The installation height of the antenna was 15 m. The water depth in the imaged area is greater than 50 m.

4 RESULTS AND DISCUSSION

The presented data cover a period of four months from 14 December 2008 to 18 April 2009. A standard radar image sequence consisting of 32 images, representing a time span of about 80 s, was used to calculate sea state parameters and sea surface current. The sub images are 376 × 913 m^2 (N_x = 256, N_y = 256) in size and a location 900 m north of the antenna was chosen for the analysis. Examples of the two differently polarized radar images on March 25, 2009 at Zhangzi Island are shown (Fig.2).

4.1 Near surface current

Current speed and direction were obtained from radar datasets measured at Zhangzi Island. A comparison of the current obtained from radar imagery and current meter is shown (Fig.3). The current direction was approximately from the northeast and the southwest (Fig.3c, d). Note that the correlations of current directions measured between the two polarized radars and buoy are quite high.

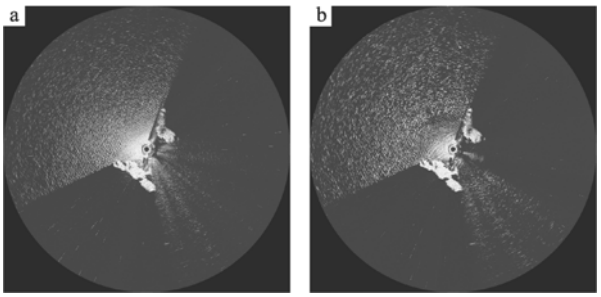

Fig.2 Two different polarization radar images on March 25, 2009

The left image taken at 08:49 is VV polarized. The right image taken at 08:53 is HH polarized

However, the correlation of current speed measured between the VV polarization radar and buoy is higher than between the HH polarization radar and buoy. In addition, the standard deviations of the current speed and direction obtained from the VV polarized radar imagery are smaller than those from the HH polarized radar imagery.

4.2 Significant wave height

In this study, the radar datasets were acquired during two separate field campaigns. As mentioned previously, the data used for calibration were collected at Zhangzi Island from February to April 2009. The process of the calibration was carried out by the method described above and results are shown in Fig.4. It was shown that the correlation coefficients for measurements made by buoy and those retrieved from radar are high and that those for VV polarizations are higher than for HH polarization. Hence, a calibrated linear model could be used to calculate significant wave height.

The validation datasets were collected at Zhangzi Island during January 2009 and in SCS on 26 June 2009. Fig.5 shows a typical example of the results, and it provides a validation of the estimation of wave height using a linear model. During January 2009, the values of the measured significant wave height varied between 0.4 and 1.6 m. The greater wave heights were measured by radar in the South China Sea example. The time series of significant wave height is shown in Fig.5c, with a maximum value of 3.8 m. Unfortunately, no reference data were available for this period (Fig.5c).

4.3 Average wave periods

The wind at sea was dominant and the mean wave period measured at the buoy had values between 3 and 6 s during the period of our observations. Fig.6 compares the average wave periods from the buoy and the radar. The specific polarization appears to have little influence on the mean periods.

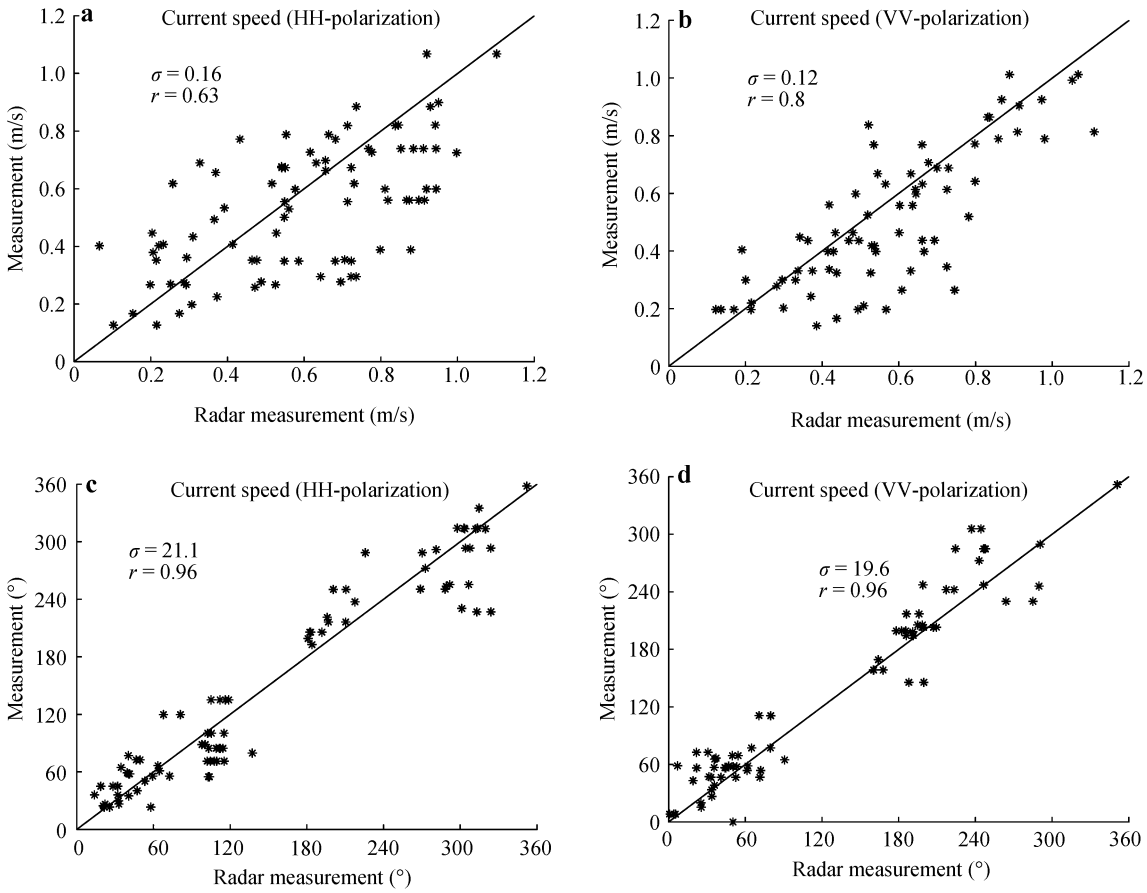

Fig.3 Scatter plot of the current speed (a and b) and current direction (c and d) from dual-polarization radar and the in-situ sensor

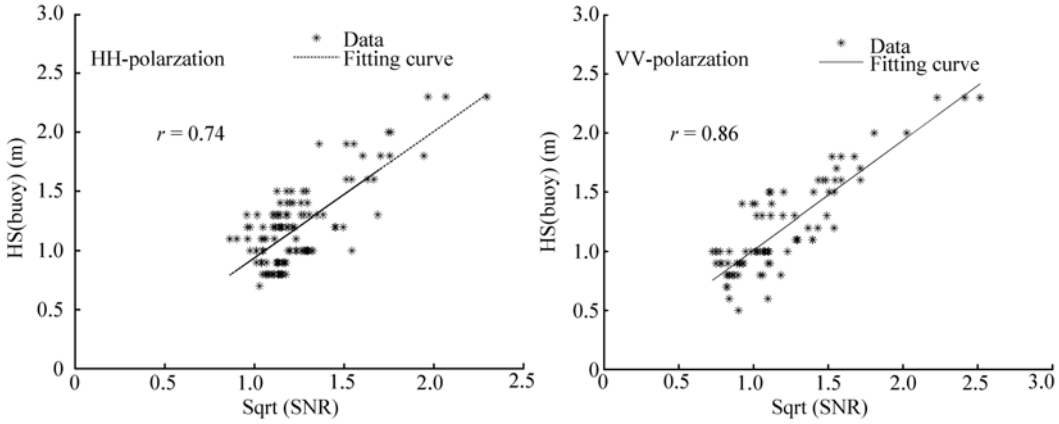

Fig.4 Linear least-square fit of Hs versus $SNR^{1/2}$ for two polarizations

4.4 Dominant wave directions

The wind directions were mainly from either the northeast or the southwest, corresponding to waves coming from these directions. The dominant wave directions estimated from buoy and radar spectra are shown in Fig.7. The calculated wave directions from the northeast seem less accurate. This phenomenon occurs because of the influence of field area topography.

During winter, the wind directions are usually from the southwest or northeast. Fig.8 gives the resulting scatter plot of the in situ wave direction versus radar-retrieved wave direction. Their correlation coefficients are very high for both HH and VV polarizations.

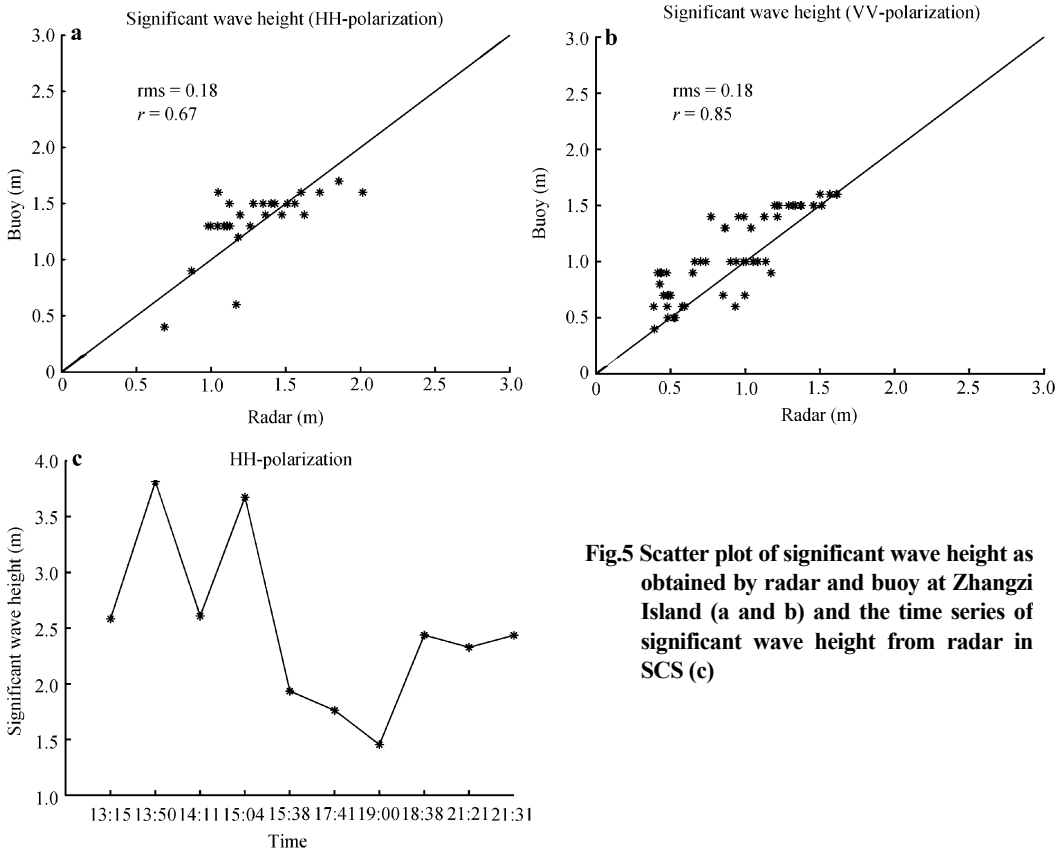

Fig.5 Scatter plot of significant wave height as obtained by radar and buoy at Zhangzi Island (a and b) and the time series of significant wave height from radar in SCS (c)

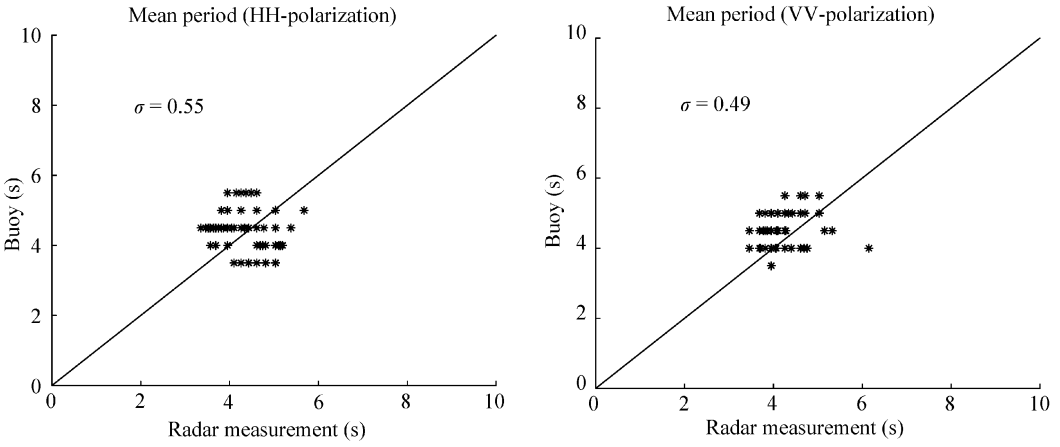

Fig.6 Scatter plot of the mean period calculated using the dual polarized radar and by the buoy

The error statistics for retrieval results are summarized in Table 1. The correlation coefficients and standard deviations for VV polarization are seen to be better than for HH polarization.

5 CONCLUSIONS

In this paper, ocean wave parameters and sea surface current information were retrieved from polarized radar imagery experiments in the Yellow Sea and South China Sea. Coincident reference sensors were used to estimate our results. This work confirmed that the radar system is effective for estimating sea state parameters and sea surface current.

A comparison of wave information and current field retrieved from dual polarized X-band nautical radar with similar information from reference sensors was performed. Radar-derived wave parameters and current information are in agreement with those measured by the reference sensor. Moreover, it is observed that the results derived from vertically-polarized radar are better than those from

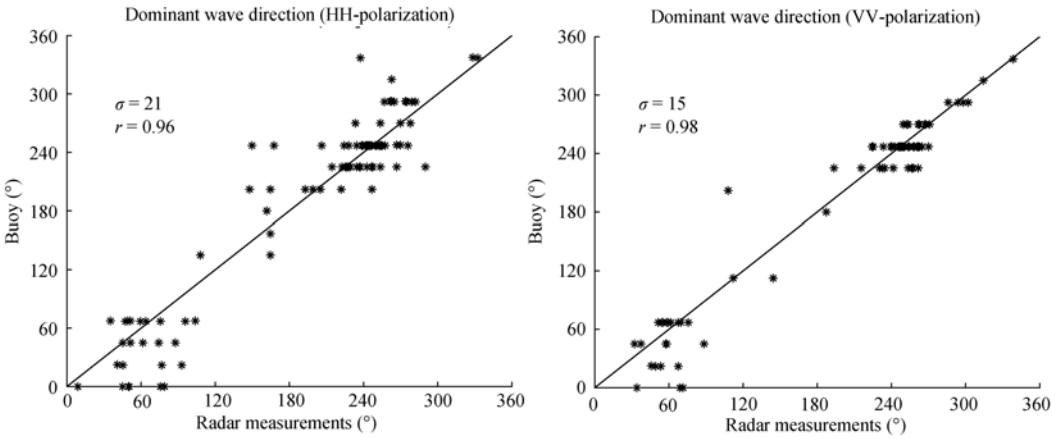

Fig.7 Scatter plot of the dominant wave direction from the dual-polarization radar and the buoy

Table 1 Error statistics of dual-polarization radar

Wave parameters and current	Standard deviation		Correlation coefficient	
	HH	VV	HH	VV
Dominant wave direction	21°	15°	0.96	0.98
Significant wave height	0.18 m	0.18 m	0.67	0.85
Average wave period	0.55 s	0.49 s	–	–
Current speed	0.15 m/s	0.12 m/s	0.63	0.80
Current direction	21.1°	19.4°	0.96	0.96

horizontally-polarized radar. In particular, it was shown that vertical polarization radar has better ability to detect significant wave heights below 1 m. Therefore, in general, vertically-polarized radar is more suitable for the measurement of the ocean wave parameters and sea surface current information.

References

Brown G S. 1998. Guest editor-special issue on low-grazing angle backscatter from rough surfaces. *IEEE Trans. Antennas Propag.*, **46**(1): 1-2.

Bell P S 1999. Shallow water bathymetry derived from an analysis of X-band marine radar images of waves. *Coastal Engineering*, **37**(3-4): 513-527.

Bell P S. 2001. Determination of bathymetry using marine radar images of waves. The 4th International Symposium on Ocean Wave Measurement & Analysis, San Francisco, USA, p. 251-257.

Bell P S, Williams J J, Clark S et al. 2006. Nested radar systems for remote coastal observations. *Journal of Coastal Research*, S139 (Proceedings of the 8th International Coastal Symposium, Itajai, S C. Brazil, 14-19 March). p. 483-487.

Borge J N, RodrIguez G R, Hessner K et al. 2004. Inversion of marine radar images for surface wave analysis. *Journal of Atmospheric and Oceanic Technology*, **21**: 1 291-1 300.

Dankert H, Horstmann J, Lehner S et al. 2003. Detection of wave groups in SAR images and radar-image sequences. *IEEE Trans. Geosci. Remote Sens.*, **41**(6): 1 437-1 446.

Dankert H. 2003. Retrive of surface-current fields and bathymetries using radar-image sequences. Proce. Int. Geosci. Remote Sens. Symp. p. 2 671-2 673.

Dankert H, Horstamann J, Rosenthal W. 2004. Ocean surface winds retrieved from marine radar image sequences. Proce. Int. Geosci. Remote Sens. Symp. Anchorage, Alaska. p. 20-24.

Dankert H, Horstmann J, Rosenthal W. 2005. Wind- and wave-field measurements using marine X-band radar-image sequences. *IEEE Journal of oceanic engineering,***30**(3):534-542.

Doong D J, Wu L Ch, Kao Ch Ch et al. 2003. Wavelet spectrum extracted from coastal marine radar images. Proce. The 13th Int. Offshore and Polar Engineering. Honolulu, Hawaii, USA. p. 258-264

Forget P, Saillard M, Broche P. 2006. Observations of the sea surface by coherent L band radar at low grazing angles in a nearshore environment. *Journal of Geophysical Research*, **111**(C0): 9 015-9 028.

Gangeskar R. 2002. Ocean current estimated from X-band radar sea surface images. *IEEE Transactions on Geoscience and Remote Sensing*, **40**(4): 783-792

Hwang P A, Sletten M A, Toporkov J V. 2008a. Analysis of radar sea return for breaking wave investigation. *Journal of geophysical research*, **113**(C0): 2 003-2 018.

Hwang P A, Sletten M A, Toporkov J V. 2008b. Breaking wave contribution to low grazing angle radar backscatter from the ocean surface. *Journal of Geophysical Research*, **113**(C0): 9 017-9 028.

Lee P H, Barter J D, Beach K L et al. 1995. X-band microwave backscattering from ocean waves. *Journal of Geophysical Research*, **100**(C2): 2 591-2 611.

LI J G, WANG J, CHEN Ch. 2006. Design and analysis on wave measuring system by X-band marine radar. *Ocean Technology*, **25** (2): 15-18. (in Chinese)

Nieto J C, Soares C G. 2000. Analysis of directional wave

fields using X-band navigation radar. *Coastal Engineering*, **40**: 375-391.

Ren F A, Shao M H, Sun Y W. 2006. The study of sea wave observed by shipborne radar. *Acta Oeanologica Sinica*, **28**(5): 152-156. (in Chinese with English abstract)

Seemann J, Ziemer F, Senet C M. 1997. A Method for Computing Calibrated Ocean Wave Spectra from Measurements with a Nautical X-Band Radar. Proc. Oceans'97 MTS/IEEE Conf., 500 years of Ocean Exploration, San Diego, CA. **2**. p. 1 148-1 154.

Senet C M, Seemann J, Ziemer F. 2001. The near surface current velocity determined from image sequences of the sea surface. *IEEE Transactions on Geoscience and Remote Sensing*, **39**(3): 492-505.

Trizna D B, Carlson D J. 1996. Studies of dual polarized low grazing angle radar sea scatter in nearshore regions. *IEEE Transactions on Geoscience and Remote Sensing*, **34**(3): 747-757.

Young I R, Rosenthal W, Zimmer F. 1985. A three dimensional analysis of marine radar images for the determination of ocean wave directionality and surface currents. *Journal of Geophysical Research*, **90**(C1): 1 049-1 059.

Ziemer F, Gunther H. 1994. A system to monitor ocean wave fields. Proc. Second Int. Conf. on Air-sea Interaction and Meteorology and Oceanography of the Coastal Zone, Lisbon, Portugal, Amer. Metetor. Soc. p. 18-19.